STEM CELLS AND DEVELOPMENT
Volume 25, Number 10, 2016

DOI: 10.1089/scd.2015.0345

# Differentiation of Spiral Ganglion-Derived Neural Stem Cells into Functional Synaptogenetic Neurons

Xiaoyang Li,[1] Alicia Aleardi,[2] Jue Wang,[1] Yang Zhou,[1] Rodrigo Andrade,[2] and Zhengqing Hu[1]

Spiral ganglion neurons (SGNs) are usually damaged in sensorineural hearing loss. SGN-derived neural stem cells (NSCs) have been identified and proposed to differentiate into neurons to replace damaged SGNs. However, it remains obscure whether SGN-NSC-derived neurons (ScNs) are electrophysiologically functional and possess the capability to form neural connections. Here, we found that SGN-derived cells demonstrated NSC characteristics and differentiated into SGN-like glutamatergic neurons. Neurotrophins significantly increased neuronal differentiation and neurite length of ScNs. Patch clamp recording revealed that ScNs possessed SGN-like NaV and HCN channels, suggesting electrophysiological function. FM1-43 staining and synaptic protein immunofluorescence showed ScNs possess the ability to form neural connections. Astrocyte-conditioned medium was able to stimulate ScNs to express synaptic proteins. These data suggested that neurotrophins are able to stimulate postnatal SGN-NSCs to differentiate into functional glutamatergic ScNs with the capability to form synaptic connections in vitro.

## Introduction

In the auditory system, sensory hair cells detect and convert sounds into auditory signals, which is mediated by primary cochlear afferent neurons, the spiral ganglion neurons (SGNs). The glutamatergic SGNs relay auditory information from hair cells to the brainstem via peripheral processes to hair cells and long central processes (the cochlear nerve) to the brainstem [1,2]. In mammals, hair cell loss and SGN degeneration are usually irreversible and cause permanent sensorineural hearing loss and other inner ear disorders, which affect ~10% of the population [3]. However, endogenous neuron repair after SGN damage is limited [4].

Evidences from previous studies indicate that damage to SGN usually results in dysfunction of conveying auditory signals to the brainstem. SGN damage is seen in many circumstances such as intense sound exposure, aging, head trauma, and other diseases. For example, a mouse study reported that noise-induced hearing loss caused acute loss of SGN peripheral nerve terminals within 24 h, and delayed/progressive loss of SGNs retained over months [5]. In studying the effect of aging on SGN damage using adult rats, the median number of cochlear fibers in elder rats (35–36 months old) was reduced by 24% compared to young adult rats (2–3 months old) [6]. Temporal bone trauma patients usually involve cochlear nerve damage, which causes hearing loss [7]. Additionally, SGN degeneration can also be found in many diseases such as endolymphatic hydrops, Friedreich's ataxia, Fabry's disease, and Usher syndrome [8–10]. Currently, there is no effective treatment to biologically replace damaged SGNs.

Stem cell-based cell therapy has been proposed to substitute degenerated SGNs [11]. Several potential candidate cell sources including mouse embryonic stem (ES) cells [12,13], human ES-cell-derived otic progenitors [14], olfactory-derived neural stem cells (NSCs) [15], and brain-derived NSCs [12,16] have been transplanted into the auditory system. In the in vitro studies, identification of spiral ganglion stem/progenitor cells has been studied using the culture methods that are similar to identifying NSCs in subventricular zone and subgranular zone. Our previous study showed that cells derived from mouse embryonic cochleovestibular ganglion (CVG, also called statoacoustic ganglion, SAG) proliferated, formed spheres in serum-free culture medium, and expressed NSC proteins nestin and Sox2, which indicated that NSCs may exist in these neural sphere-forming cells [17]. These embryonic CVG-derived-NSCs differentiated into cells expressing neuronal intermediate filament and tubulin, including neurofilament and β-III tubulin (TUJ1) [17]. Additionally, cells that were harvested from postnatal mouse spiral ganglion tissues were able to proliferate and form spherical structures in serum-free culture medium [18–21]. When cultured on gelatin-coated substrate and exposed to neurotrophins including brain-derived neurotrophic factor (BDNF) and neurotrophin-3 (NT-3), they were able to differentiate into cells expressing neuronal proteins neurofilament and TUJ1, or the glial cell marker glial fibrillary acidic protein (GFAP) [18,19]. However, the neuronal features

Departments of [1]Otolaryngology-HNS and [2]Pharmacology, Wayne State University School of Medicine, Detroit, Michigan.

of these SGN-NSC-derived neuron-like cells have not been fully characterized, including the neuronal subtype and the yield of neuronal differentiation. Moreover, SGNs send peripheral and central processes to connect hair cells to the cochlear nucleus in the brainstem; therefore, SGN replacement should include regenerating and characterizing neurite outgrowing from NSC-derived neurons. However, neurite outgrowth has not been studied in inner ear NSC-derived neurons. Additionally, the function of inner ear sensory epithelium-derived neurons has been reported [20], but the function of inner ear spiral ganglion-derived neurons has not been explored using electrophysiology.

In this study, in addition to identifying NSCs from postnatal mouse SGN tissues and examining how to stimulate SGN-NSCs to become numbers of neuronal-like cells [SGN-NSC-derived neurons (ScNs)], we focused on (1) characterizing the type and neurite extension of ScNs; (2) determining the functional activity of ScN using electrophysiology; and (3) investigating the synaptogenesis capability of ScNs. Characterizing the functional and synaptogenesis abilities of ScNs is critical to develop SGN replacement using ScNs as a potential cell source in the future.

## Materials and Methods

### *Generation of neurospheres from postnatal mice spiral ganglion*

Swiss Webster mice (Charles River) and EGFP transgenic mice (ACTbEGFP, JAX mice) were used in this study. The care and use of the animals have been approved by local Institutional Animal Care and Use Committee. Postnatal day 2–5 mice were decapitated and the spiral ganglia were isolated in cold Dulbecco's modified Eagle's medium (DMEM)/High glucose (Hyclone), followed by mechanical dissociation using 200 μL pipette trituration.

Dissociated cells were cultured in 24-well culture plate (Nunc) in suspension medium containing DMEM/F12, N2, B27, epidermal growth factor (EGF; 20 ng/mL), fibroblast growth factor 2 (FGF2; 20 ng/mL), and penicillin-streptomycin (all from Invitrogen) at 30%–40% confluence in 5% $CO_2$ and 37°C incubator [17]. Spiral ganglion primary cultures were observed daily using a phase contrast microscopy (Leica) and passaged every 5–7 days. During passaging, floating cell aggregates were collected using centrifugation at 200 *g* for 3 min. Pellets were treated with TryplE (Invitrogen) at 37°C for 3–5 min, resuspended in suspension medium, and cultured in the incubator. Fresh suspension culture medium was added every 2–3 days. Passage 3–6 neurospheres were used in the following studies.

### *Neural sphere characterization*

To characterize proliferation, SGN-derived spheres were dissociated and cultured in suspension as described above. 5-ethynyl-2′-deoxyuridine (EdU, 200 ng/mL) was added to suspension culture medium for 72 h. Cells were fixed in 4% paraformaldehyde at room temperature for 15 min and blocked in 5% donkey serum containing 0.5% Triton X-100 for 30 min, followed by incubation in a Click-iT™ reaction cocktail containing Click-iT reaction buffer, $CuSO_4$, Alexa-Fluor 555, and reaction buffer additive (Invitrogen) for 30 min. Nucleus were labeled by 4′,6-diamidino-2-phenylindole (DAPI). Samples were observed and imaged using Leica SPE confocal microscopy. The number of EdU-positive cells was counted in each sphere by Cell Counter plugin using ImageJ software (NIH), and (EdU-positive cells)/(DAPI-positive cells) was calculated ($n = 6$ coverslips, 7 spheres were randomly selected).

To determine whether SGN-derived spheres expressed NSC proteins, SGN-derived spheres were transferred to glass coverslips and fixed in 4% paraformaldehyde for immunofluorescence using anti-neural adhesion molecules (NCAM, sc-106; SCBT), anti-GFAP (sc-6170; SCBT), anti-A2B5 (MAB1416; R&D systems), anti-Sox2 (ab107156; Abcam), and anti-nestin (RAT-401; DSHB) antibodies. For immunofluorescence in this study, primary antibodies were incubated at 4°C overnight. Dylight488, Dylight549, or Dylight649 conjugated secondary antibodies (Jackson Immunoresearch) and appropriate filter sets were applied to observe the samples using Leica epifluorescence microscopy and/or confocal microscopy.

### *Neuronal yield and neurite outgrowth assay*

To study neuronal differentiation and test whether BDNF was able to affect the cell fate of SGN-derived neural spheres, cell suspensions were dissociated and resuspended in differentiation medium (45% Neurobasal, 45% DMEM/F12, 10% fetal bovine serum, L-glutamine, 0.1% 2-mercaptoethanol, and penicillin-streptomycin, all from Invitrogen) with or without 20 ng/mL BDNF (R&D systems). Cells were seeded to 0.1% gelatin-coated custom-made glass coverslips (5 mm in diameter) at 40% confluence and maintained for 3–5 days in the incubator (treatment period of the control and BDNF group was the same in each experiment).

In this study, anti-TUJ1 (AB9354; Millipore), anti-neurofilament (NF, sc-20012; SCBT), anti-vesicular glutamate transporter 1 (VGLUT1, MAB5502; Millipore), anti-NeuroD (sc-46684; SCBT), and anti-NeuN (MAB377; Millipore) antibodies were used to characterize neuronal maker expression. The following criteria were applied to observe and quantify neuron-like cells. First, cells had positive TUJ1 and neurofilament immunostaining. Second, typical neuronal morphology such as large, round centrally located nucleus and neurites growing outward from the soma must be observed. Third, the outgrowth of neuronal-like cells had to be longer than the diameter of the soma.

Three fields were randomly selected and observed in each coverslip by a 20× objective in the control and BDNF groups using Leica epifluorescence microscopy ($n = 6$ coverslip samples). First, all TUJ1 and DAPI-positive cells were counted for neuronal yield quantification. Neuronal yield was calculated as (TUJ1-positive cells)/(DAPI-positive cells) × 100%. To compare the yield between the control and treatment groups, normality tests was performed and two-tailed Student's *t*-test was applied. Second, the numbers of neurites extending from ScNs were observed. Difference between control and treatment ScNs on neurite number was tested by normality tests and Student's *t*-test. Third, neurite length was calculated using ImageJ by setting up a scale and tracing the path of neurite outgrowth. Normality tests and Student's *t*-test was used to compare the neurite length of treated and control ScNs. In all statistical analyses, normality tests were performed with SPSS Statistics (IBM) and Student's *t*-tests were applied in normally distributed data.

### Electrophysiology

Passages 3–6 SGN-derived spheres were dissociated with TryplE and single cells were plated on glass coverslips with culture medium containing DMEM/F12, neurobasal medium, 10% fetal bovine serum (FBS), and BDNF (20 ng/mL) for 3–5 days before electrophysiology analysis. Coverslips were placed in a recording chamber on the stage of an Olympus BX50 microscope where they were superfused with Ringer's solution bubbled to saturation with 95% $O_2 + 5\%$ $CO_2$ and maintained at $30° \pm 1°C$ (Ringer composition in mM: 119 NaCl, 2.5 KCl, 1.3 $MgSO_4$, 2.5 $CaCl_2$, 1 $NaH_2PO_4$, 26.2 $NaHCO_3$, and 11 glucose). Control experiments on cortical neurons in brain slices were conducted essentially as described previously [22]. Cells were imaged using differential interference contrast (DIC) and targeted for recording based upon their morphology.

Electrical signals were recorded using an EPC10 Amplifier (HEKA) under the control of Patchmaster v.2 × 69. Recording pipettes were pulled from borosilicate glass (outer diameter, 1.2 mm) using a Flaming-Brown P-97 horizontal puller (Sutter Instruments) to give resistance ranging from 2 to 4 MΩ when filled with a potassium-based intracellular recording solution containing (in mM) the following: 130 $KMeSO_4$, 5 KCl, 5 NaCl, 0.02 EGTA, 1 $MgCl_2$, 10 $Na_2$ phosphocreatine, 4 ATP, 0.3 GTP, and 11 HEPES, pH 7.3–7.4. Series resistance typically ranged 10–15 MΩ was left uncompensated in the voltage clamp experiments. Resting membrane potential and membrane input resistance were assessed immediately after breaking into the cells. Input resistance was measured using 50–100 pA hyperpolarizing pulses from rest and the ability of the cells was tested using constant current depolarizing steps after bringing the cell to −60 to −70 mV using constant current injection.

### Synaptic protein assay

Expression of synaptic proteins was examined to determine whether ScNs had the potential to form synapses. SGN spheres were dissociated with TryplE and seeded to glass coverslip at 30%–40% confluence containing differentiation medium in the presence of 20 ng/mL BDNF (control). Cells were observed daily for 6–9 days and half of the medium was replaced every 3 days. FM1-43FX (FM1-43; 2.5 nM diluted in HBSS; Invitrogen) was applied to SGN neurons (positive control, data not shown) and ScNs. The experimental recorded image was obtained through an inverted Leica epifluorescence microscope for 3–10 min. Images were taken under DIC and corresponding fluorescence channel under a 20× objective.

Astrocyte-conditioned medium (ACM) was obtained from the cortex of postnatal day 0–1 Swiss Webster pups. Cortex tissues were isolated, dissociated by pipetting, and cultured in 90% DMEM High glucose, 10% FBS, and penicillin-streptomycin (all from Hyclone). Cultures were observed under light microscope daily. When cells reached 60%–70% confluence, they were dissociated with TryplE and resuspended in the fresh culture medium. During cortex cell passaging, a small amount of cells were seeded to gelatin-coated coverslips for TUJ1, MOG (AB5692; Millipore), and GFAP staining. At passage 2 (∼2 weeks after primary culture), all cells were GFAP positive and we collected ACM after this passage for 4–5 passages. Collected conditioned medium was filtered with a 0.45 μm filter (Millipore) to remove cell debris. 30 kDa molecular weight cutoff tubes (Millipore) were used to concentrate ACM using the manufacturer's protocol. Concentrated ACM was filtered with 0.22 μm syringe filters (Millipore) and stored at −20°C. ACM was added to the culture medium at the ratio of 1:10.

SGN spheres were dissociated with TryplE, seeded to glass coverslips at 30%–40% confluence, and pretreated with the BDNF-containing differentiation medium (control medium) for 2 days, followed by treatment of either control medium or ACM medium (ACM was added to the control medium) for additional 4–7 days. The ACM and control group were treated for a total of 6–9 days, and in each experiment two groups were treated for the same period. At the end of the culture, samples were fixed and proceeded for immunofluorescence using antibodies specific for anti-synaptic vesicles (SV2, SV2-a; DSHB), anti-post synaptic density 93 (PSD 93, 73–057; NeuroMab), and anti-synapsin I (sc-20780; SCBT).

For analysis, expression of synaptic protein SV2 was used to evaluate the synaptogenesis capability of ScNs. The SV2 puncta area, which was determined as 0.4–3 $\mu m^2$ in size, was quantified by ImageJ (NIH) using the particle analyze feature with color threshold. In each sample, the SV2 puncta area per TUJ1-expressing neuron was calculated in the control and ACM group ($n = 25$ in the control and $n = 26$ in the ACM groups, from four independent experiments, 5–7 samples per experiment) and presented as mean ± standard deviation. Additionally, the number of SV2 puncta per TUJ1-expressing neuron was counted using color threshold in ImageJ. Normality test was performed by SPSS, Mann–Whitney $U$ test was applied to this set of data. $P < 0.05$ was considered statistically significant.

### Immunoblot

To test whether BDNF expressed in ACM, DMEM/F12, U87 (sc-2411, positive control of BDNF; SCBT), and ACM were fractionated by 12% precast SDS PAGE gels and transferred onto polyvinylidene difluoride (PVDF) membrane according to manufacturer's protocols (Bio-Rad). Blots were blocked with 5% TBST-milk for 60 min. Primary antibody was rabbit anti-BDNF (sc-2098, 1:200; SCBT) with HRP-conjugated goat anti-rabbit secondary antibodies (1:2000; Thermo Scientific). Signals were visualized by a commercial chemiluminescence kit (SuperSignal™ Chemiluminescent HRP Substrates, Thermo Scientific) according to the manufacturer's protocol.

## Results

### Postnatal mouse SGN-derived cells were able to form spheres and express NSC markers

In the primary culture of postnatal SGN, dissociated cells formed small cell aggregates in 1–2 days in serum-free medium. After 2–3 days, cell aggregates became larger and finally formed spherical structures in 4–6 days (Fig. 1A). To study cell proliferation and sphere formation ability, primary culture spheres were dissociated into single cells, and we found that these single cells were able to form spherical cell aggregates in 4–6 days (Fig. 1B). In this study, postnatal SGN-derived cells were able to be passaged to form spherical aggregates for at least 5–7 passages. To characterize the

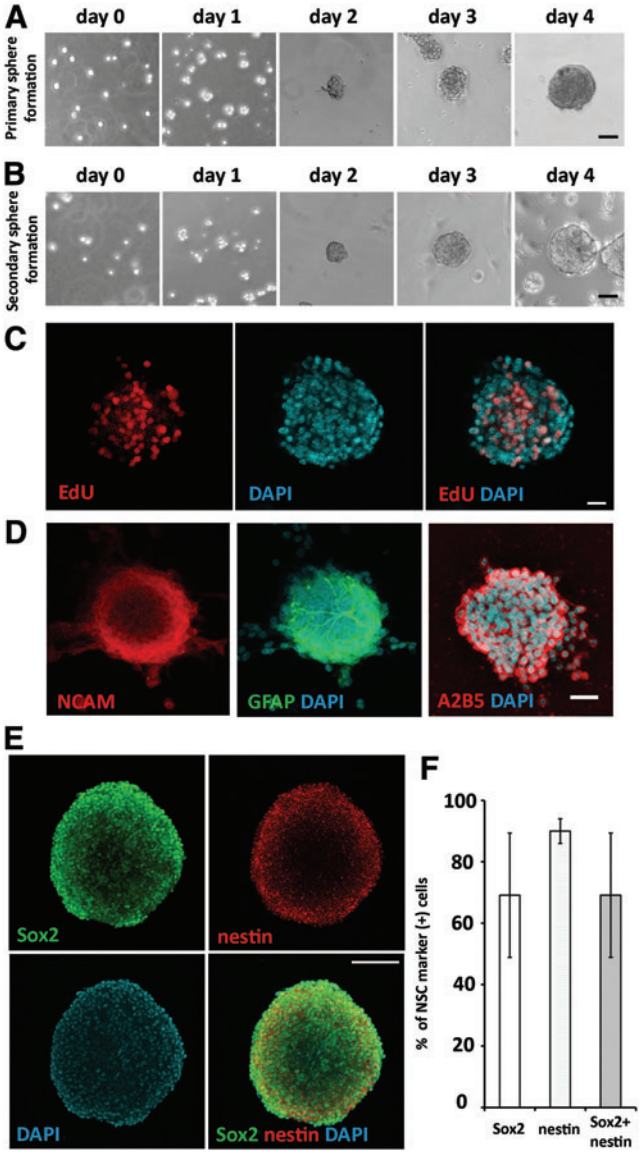


**FIG. 1.** SGN-derived cells were able to form spheres and express NSC markers. **(A)** Dissociated single cells from postnatal day 2 mouse SGN formed cell clusters and spheres in serum-free medium in 4 days. **(B)** Single cells dissociated from primary SGN-derived spheres formed cell clusters and grew into spheres in 4 days. **(C)** Confocal microscopy images showed that passage 2 SGN spheres incorporated EdU after exposure to EdU for 72 h. **(D)** Confocal microscopy images showed the expression of neural stem cell marker NCAM, GFAP, A2B5. **(E)** Passage 4 SGN spheres expressed NSC markers Sox2 and nestin (confocal microscopy). Majority cells expressed both Sox2 and nestin, whereas a few cells only expressed Sox2. **(F)** The percentages of Sox2 positive, nestin positive, and Sox2/nestin positive were 65.54% ± 23.31%, 90.41% ± 4.8%, and 65.54% ± 23.31%, respectively ($n = 5$; mean ± standard deviation). Scale bar: 50 μm in **(A, B)**; 20 μm in **(C)**; 30 μm in **(D)**; 100 μm in **(E)**. GFAP, glial fibrillary acidic protein; NSC, neural stem cells; SGNs, spiral ganglion neurons. Color images available online at www.liebertpub.com/scd

proliferation of SGN-derived cells, cells were cultured in suspension in the presence of EdU for 72 h, followed by fixation, EdU staining, and confocal microscopy. It was found that these cells were able to incorporate EdU (Fig. 1C). Quantitative study showed that ~43.26% ± 18.22% (mean ± standard deviation) SGN-derived cells incorporated EdU after 72 h in the culture ($n = 7$ neurospheres).

To determine whether SGN-derived sphere-forming cells expressed NSC markers, passage 4–5 SGN-derived spheres were fixed for immunofluorescence using anti-NCAM, anti-GFAP, anti-A2B5, anti-Sox2, and anti-nestin antibodies. Confocal microscopy 3D reconstitution (Fig. 1D, E) showed that SGN spheres expressed NCAM, GFAP, A2B5, Sox2, and/or nestin. It was found that 35.40% ± 10.67% (mean ± standard deviation) NCAM positive, 24.98% ± 18.65% GFAP positive, and 47.91% ± 9.08% A2B5 positive cells were detected respectively ($n = 6$ for each marker). Quantitative study revealed that ~65.54% ± 23.31% cells were nestin positive, 90.41% ± 4.8% were Sox 2 positive ($n = 5$; Fig. 1F), and all nestin positive cells were double labeled by anti-Sox2 antibodies. These data indicated that postnatal SGN-derived cells expressed NSC proteins; therefore, they were likely NSCs (SGN-NSCs).

### *BDNF stimulated neuronal differentiation of SGN-NSCs*

We investigated whether postnatal SGN-NSCs were able to differentiate into cells expressing neuronal markers. In adherent culture (Fig. 2A diagram), NSCs were able to attach, spread, and differentiate into cells showing neuronal morphology on light microscopy (refer to Figs. 4A and 6A). At the end of the culture (Fig. 2A diagram), samples were fixed and immunofluorescence showed that expression of nestin was decreased by confocal microscopy (Fig. 2A). Quantitative study showed 9.2% ± 3.8% (mean ± standard deviation) nestin-positive cells were observed when ScN differentiated ($n = 4$ coverslips). Additionally, SGN spheres differentiated into cells expressing neuronal proteins TUJ1, NF, VGLUT1, NeuroD, and NeuN (Fig. 2B).

To characterize the yield of ScNs that derived from SGN-NSCs, passage 3–5 SGN-NSC spheres were dissociated and maintained in adherent culture, followed by TUJ1/DAPI staining to indicate the number of neuron-like cells/total number of cells. We found that the yield of ScNs expressing TUJ1 was low (Fig. 2C). To increase the yield of ScNs, BDNF was added to culture medium for 3–5 days. Immunofluorescence showed that 47.63% ± 7.93% (mean ± standard deviation) of SGN-NSCs differentiated into ScNs in the BDNF group, whereas it was 29.48% ± 9.28% in the control group without BDNF supplementation (Fig. 2D). Student's *t*-test indicated statistically significant difference ($P < 0.01$, Student's *t*-test; $n = 6$ coverslips). Overall, BDNF was able to promote neuronal differentiation of postnatal mouse SGN-NSCs.

Because mature mouse SGNs are glutamatergic neurons, we characterized the yield of glutamatergic neurons by studying the expression of VGLUT1/TUJ1 using immunofluorescence. We found that 95.7% ± 5.5% (mean ± standard deviation) TUJ1-positive cells were also VGLUT1 positive in the control group, whereas the number was 98.24% ± 3.34% (mean ± standard deviation) in BDNF-treated cultures

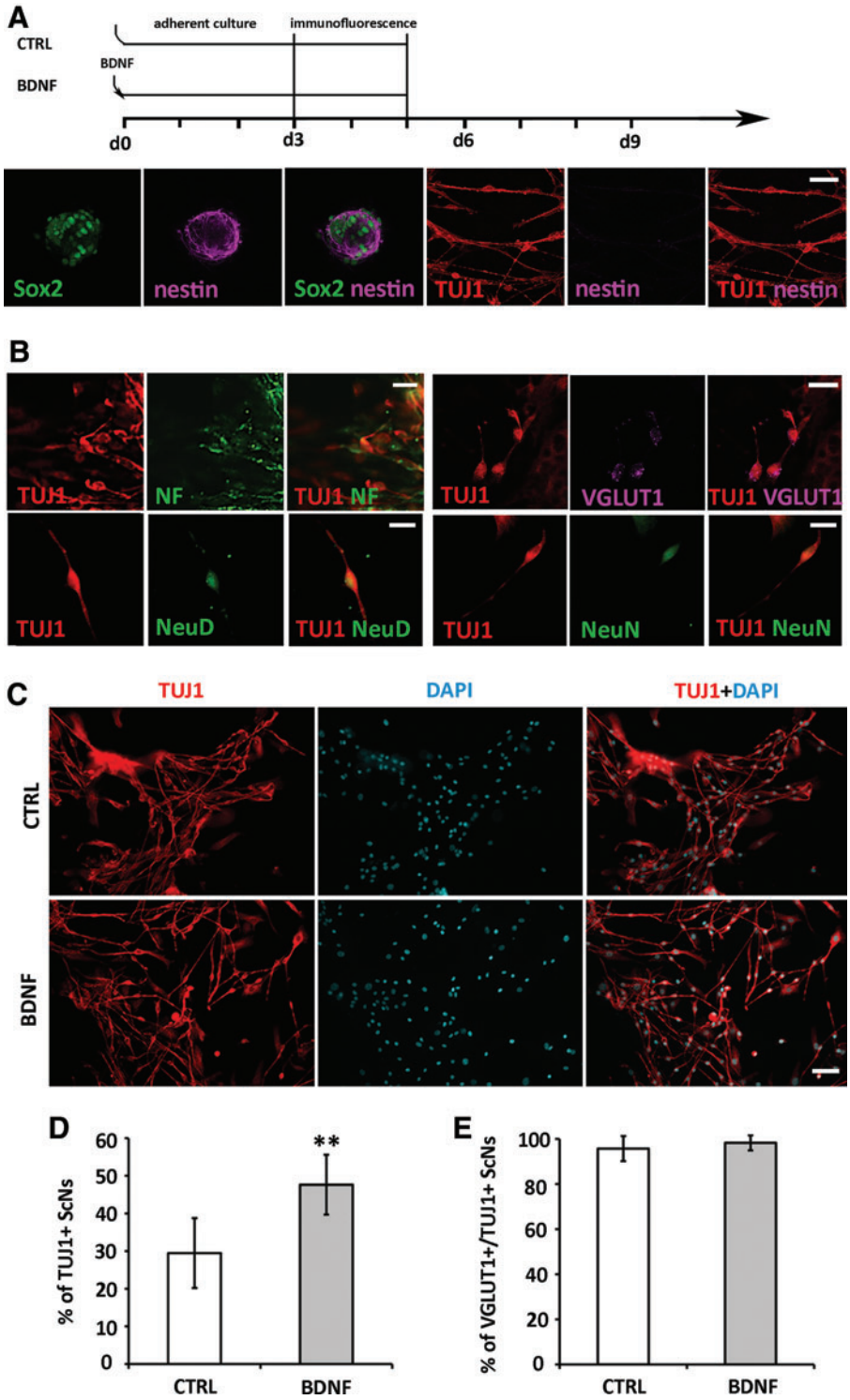


**FIG. 2.** SGN-NSCs differentiated into glutamatergic neurons. **(A)** Diagram showed ScN differentiation in adherent culture: BDNF was added to differentiation medium on day 0 whereas control (CTRL) group only used the differentiation medium. Cells were maintained for the same time period for 3–5 days in both groups and then fixed and proceeded immunostaining. ScNs expressed neural stem cells markers Sox2 and nestin whereas nestin expression was decreased when ScNs differentiated. **(B)** Cells derived from SGN spheres expressed neuron markers βIII-tubulin (TUJI), NF, NeuroD (NeuD), NeuN, and glutamatergic neuron marker VGLUT1. **(C)** Passage 3 SGN spheres were cultured in adherent cultures for 3 days. TUJ1-positive cells were found in the absence (*upper panels*, CTRL) and presence of BDNF (*lower panels*, BDNF). **(D)** In quantitative analysis, ScNs treated with BDNF had significantly more TUJ1-positive cells than the control group (**$P<0.01$; Student's *t*-test). **(E)** Quantitative analysis indicated no significant differences on VGLUT1-positive neurons between the control and BDNF-treated groups ($n=6$, $P>0.05$, Mann–Whitney *U* test). Scale bar: 50 μm in **(A)**, 20 μm in **(B)**; 50 μm in **(C)**. BDNF, brain-derived neurotrophic factor; NF, neurofilament; ScNs, SGN-NSC-derived neurons. Color images available online at www.liebertpub.com/scd

(Fig. 2E). Mann–Whitney *U* test indicated no statistical significance ($P>0.05$, $n=6$ coverslips).

To examine whether BDNF was able to stimulate generation/initiation of neurite projections, the number of neurites was counted in ScNs. No significant difference was identified in the number of neurite outgrowth per neuron between the control and BDNF groups ($P>0.05$, Student's *t*-test; $n=6$ coverslips; Fig. 3A, B). To determine whether BDNF was able to promote the extension/elongation of neurite outgrowth from ScNs, we added BDNF to the culture medium. We found that the length of neurite outgrowth in the BDNF group ($153.96\pm16.61$ μm; mean ± standard deviation) was significantly longer than the control group ($93.38\pm15.78$ μm; $P<0.001$, Student's *t*-test; $n=6$ coverslips; Fig. 3C). Overall, it appeared that BDNF enhanced ScN-derived neurite outgrowth in length but not in quantity.

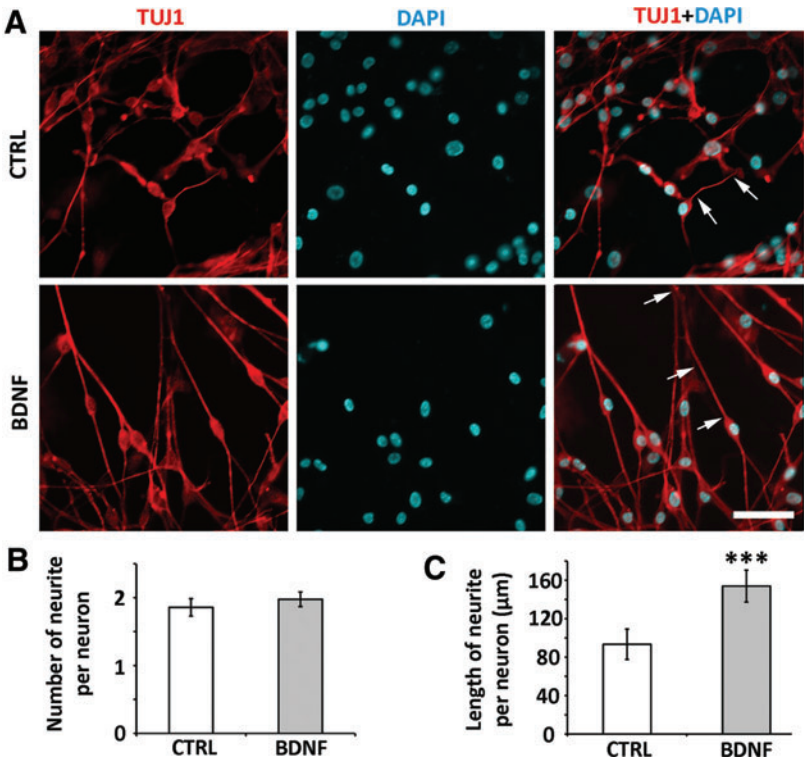


**FIG. 3.** BDNF promoted SGN-NSC neurite elongation but not the number of neurite outgrowth. **(A)** The neuron cell body and neurite outgrowth were labeled by TUJ1 immunostaining in the control (*upper panels*, CTRL) and BDNF treated (*lower panels*, BDNF) ScNs. **(B)** Quantitative analysis indicated that the number of ScNs neurite outgrowths in the control group was not significantly different from that in the BDNF treatment group ($P > 0.05$, Student's *t*-test). **(C)** The neurite length of TUJ1-positive ScNs in the BDNF treatment group was $153.96 \pm 16.61$ μm, whereas it was $93.38 \pm 15.78$ μm in the control group ($n = 6$, $^{***}P < 0.001$, Student's *t*-test, arrows indicated representative neurites). Scale bar: 25 μm in **(A)**. Color images available online at www.liebertpub.com/scd

### *ScNs showed neuron excitability in electrophysiology*

To study whether ScNs were electrophysiologically functional, passage 3–6 SGN-NSCs were treated with BDNF for 3–5 days. We sampled the excitability of ScNs ($n = 18$ cells from 4 samples) using patch clamp recordings and found that cells characterized by their round soma consistently fired overshooting action potentials in response to constant current depolarizing steps ($n = 9$ cells, Fig. 4A, B). These cells exhibited a resting membrane potential of $-53.3 \pm 2.5$ mV (mean ± standard error) and an input resistance of $332 \pm 49.7$ MΩ and exhibited relatively consistent electrophysiological properties. Most notably these cells fired generally one or a few action potentials that were followed by a prominent transient ''sag'' in the voltage trajectory elicited by constant hyperpolarizing current injection (Fig. 4B). The spiking and voltage ''sag'' are similar to those of native SGN as reported in previous studies [23,24]. Administration of tetrodotoxin (TTX, 1 μM) reduced the amplitude of the action potential only slightly in two out of three tested cells but nearly blocked in the third cell. Administration of TTX to cortical neurons in brain slices in a parallel experiment completely suppressed action potential generation (Fig. 4C). These results suggested that action potential generation in ScNs involved TTX sensitive and TTX insensitive sodium channels.

The presence of a voltage ''sag'' in response to hyperpolarizing constant current pulses suggested that ScNs may

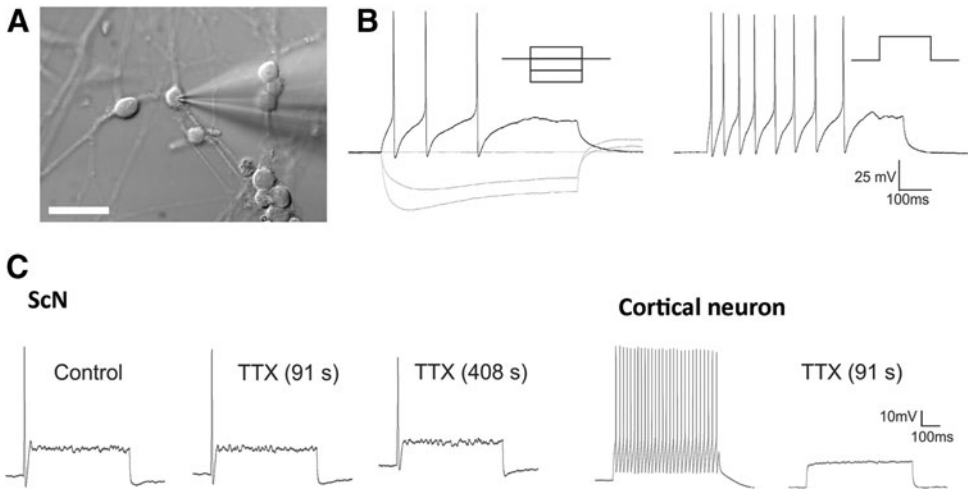


**FIG. 4.** ScNs showed neuronal excitable properties. **(A)** DIC image illustrated morphology of ScN targeted for recording. Electrically excitable cells typically exhibited a characteristic round soma. **(B)** Voltage trajectories in response to constant current hyperpolarizing pulses (−100 pA to +100 pA). **(C)** Administration of TTX had little effect of action potentials in ScNs (*left panel*) but completely suppressed them in a cortical neuron tested under the same conditions (*right panel*, positive control). Scale bar: 50 μm in **(A)**. DIC, differential interference contrast.

express HCN channels capable of generating an $I_h$ current. Since native SGNs express HCN channels and a prominent $I_h$ current [24–26], we next tested this possibility in voltage clamp experiments. As illustrated in Fig. 5A, hyperpolarizing steps from −60 mV resulted in the development of slow inward relaxations ($n = 6$ cells) that could be reversibly blocked by administration of cesium (3 mM, $n = 3$ cells, Fig. 5A). This inward relation was voltage dependent in the −60 to −120 mV range consistent with the development of a current mediated by HCN channels ($n = 3$ cells, Fig. 5B). $I_h$ currents formed by different HCN subunits differ in their kinetics [27]. As illustrated in figure the inward relaxation elicited by hyperpolarizing steps from −60 to −100 mV was well fitted by a double exponential with time constants of 137 and 800 ms, respectively, with the slower component generally being quantitatively larger (Fig. 5C). These results suggest that $I_h$ in ScNs, as in native spiral ganglia, involves the kinetically slower HCN subunits.

### *ACM stimulated ScNs to express synaptic proteins*

To study whether ScNs expressed synaptic proteins and showed synaptogenesis abilities, FM1-43-based synaptic vesicle staining assay were performed. FM1-43 has been used for vesicle recycling including synaptic vesicle recycling [28]. In this study, synaptic vesicles of ScNs were monitored by FM1-43 synaptic vesicle staining using passage 4–5 ScNs cultured in the BDNF-containing differentiation medium. It was found that positive staining was detected upon observation from 3 to 10 min following FM1-43 exposure. The neurites and soma excluding the nucleus were labeled by FM1-43 in ScNs, whereas non-neuronal cells were not stained or weakly stained (Fig. 6A). Additionally, puncta FM1-43 staining was identified along the neurites of ScN, suggesting that ScNs may express synaptic vesicles along the neurites.

In cortex primary culture, almost all surviving cells were GFAP positive after passage 2 (Fig. 6B). ACM was collected after this passage. To study whether ACM was able to stimulate synaptic vesicle protein expression, first we investigated whether ACM contained BDNF, and our western blotting showed that BDNF protein was not detected in ACM (Fig. 6B). Second, we treated ScNs with either continuous control medium (differentiation medium containing BDNF, control group) or control medium followed by ACM-containing medium (ACM added to BDNF medium; ACM group) (Fig. 6C diagram). Immunofluorescence showed SV2-positive punctae mainly on the cell body and along neurite outgrowths (Fig. 6C, arrows). Very few punctae were observed in the control group, whereas significantly increased number of SV2-positive punctae were found in the ACM group (Fig. 6C). The criteria for puncta size was 0.4–3 $\mu m^2$; however, several small punctae sometimes merged to a large puncta (>3 $\mu m^2$ and beyond the criteria) that were hard to distinguish using the ImageJ software; therefore considered as one puncta. There were totally four such large punctae in the ACM group but none in the control group. Quantitative analysis showed less punctae per ScN in the control group

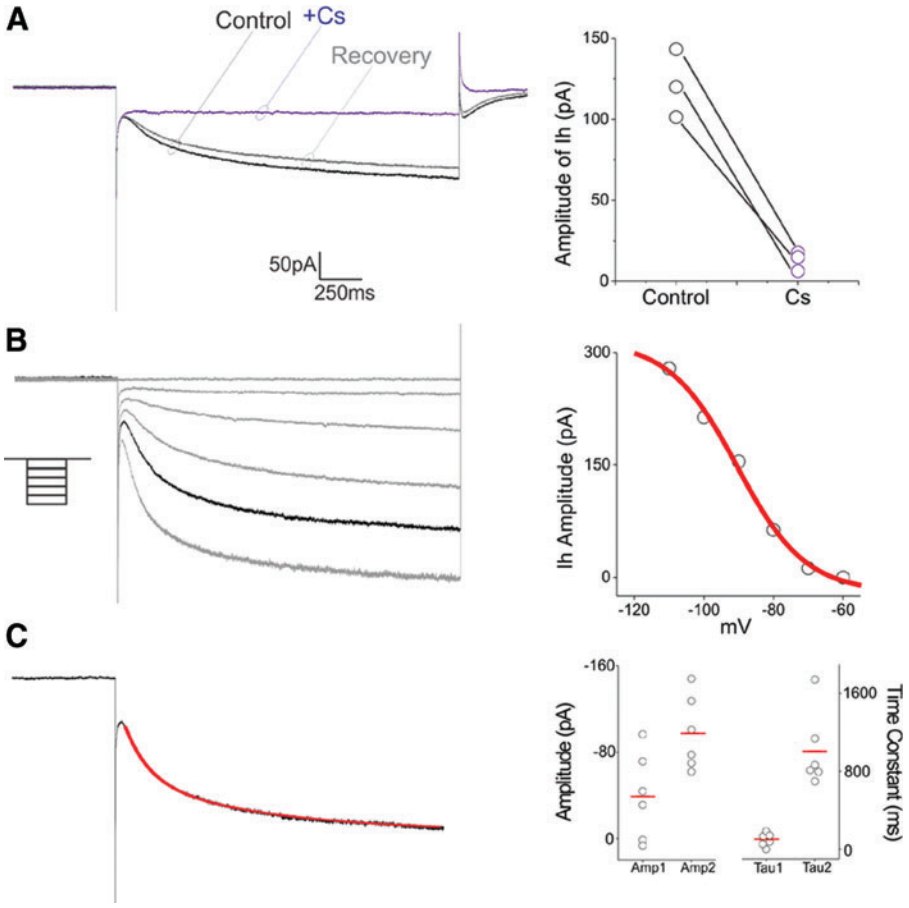


**FIG. 5.** ScNs showed HCN channels. **(A)** In voltage clamp, hyperpolarizing step from −60 to −90 mV resulted in the development of a slow inward current. This current was reversible blocked by cesium, identifying it as mediated by HCN channels (ie, $I_h$). **(B)** Voltage dependence of $I_h$ was determined using 2-sec long steps from −60 to −110 mV. **(C)** The kinetics of $I_h$ in ScNs was well fitted by two exponentials (*red line*), suggesting the presence of two components to the current, a smaller fast component and a larger slower component. Amp 1 and Amp 2 correspond to the amplitude of these two components and Tau1 and Tau 2 to their time constants. Color images available online at www.liebertpub.com/scd

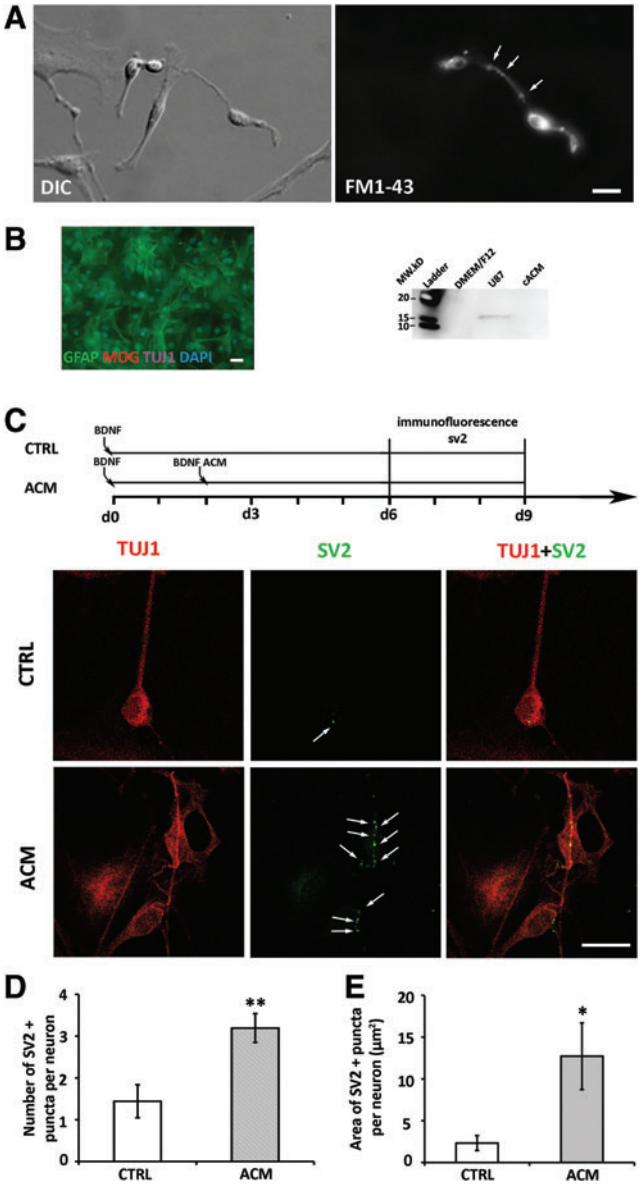


**FIG. 6.** ACM stimulated ScNs to express synaptic proteins. **(A)** SGN-derived NSCs showed various morphologies under DIC (*left*). FM1-43 stained two neuron-like cells (*right*), while non-neuron like cells were not labeled. Additionally, puncta staining (*arrows*) was found along the neurites of a bipolar neuron-like cell. **(B)** Immunostaining of TUJ1, GFAP, and MOG on passage 3 primary mouse cortex culture used for ACM collection, most cells were GFAP positive. Western blotting analysis of ACM by BDNF antibody showed band on positive control U87 but not on the ACM lane. **(C)** Diagram showed at experimental day 2 BDNF-induced ScNs were exposed to the control medium or to ACM medium. SV2 immunostaining showed puncta staining in the control and ACM groups. Arrows indicate puncta staining. **(D)** In quantitative study, the number of SV2-positive puncta in the control group was significantly lower than the ACM treatment group (**$P < 0.01$, Student's *t*-test). **(E)** In quantitative analysis of the area of SV2-positive staining, the total area of SV2 puncta in the control was significantly smaller than that in the ACM treatment group (*$P < 0.05$, Mann–Whitney *U* test). Scale bar: 20 μm in **(A–C)**. ACM, astrocyte-conditioned medium. Color images available online at www.liebertpub.com/scd

(1.44 ± 0.40, mean ± standard error) compared to the ACM group (3.19 ± 0.35; $P < 0.01$, Student's *t*-test; samples were from four independent studies, $n = 25$ in the control cultures, $n = 26$ in the ACM cultures; Fig. 6D). Moreover, the total SV2 puncta area per neuron in the ACM group (12.71 ± 3.98 $\mu m^2$, mean ± standard error) was significantly larger than the control group (2.32 ± 0.90 $\mu m^2$; $P < 0.001$, Mann–Whitney *U* test; $n = 25$ in the control group, $n = 26$ in ACM group; samples were from four independent studies; Fig. 6E).

To further determine whether synaptic structures of ACM-treated ScNs expressed both pre- and postsynaptic proteins, presynaptic antibody anti-synapsin and postsynaptic antibody anti-PSD 93 were used, and confocal microscopy showed positive pre- and postsynaptic antibody staining (Fig. 7). Moreover, 68.1% of pre- and postsynaptic punctae were colocalized on ScNs in Pearson's R test (Leica LAS AF Lite Co-localization software), indicating the potential of synaptogenesis. These data indicate that (1) ScNs were capable of expressing synaptic proteins SV2, synapsin, PSD 93, and showing the potential of neural connection formation; and (2) ACM increased the expression of synaptic proteins on ScNs.

## Discussion

In this study, we investigated the differentiation, neurite outgrowth, function, and synaptic protein expression of ScNs. We identified postnatal mouse SGN-NSCs and found

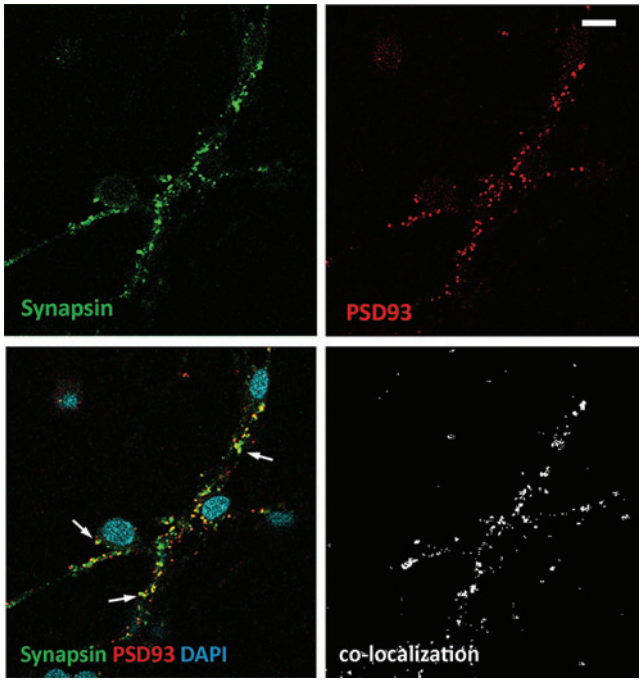


**FIG. 7.** Colocalization of pre- and postsynaptic proteins in ACM treated ScNs Immunostaining of ScNs for colocalization of presynaptic synapsin (*green*) and postsynaptic PSD 93 (*red*) showed synaptic puncta colocalization (*arrows* in the merged image) in ACM-treated ScN cultures. Image of Pearson's R test showed colocalization of synapsin and PSD93 using Leica LAS AF Lite Colocalization software. Scale bar: 10 μm. Color images available online at www.liebertpub.com/scd

that postnatal SGN-NSCs were able to proliferate, express NSC markers NCAM, GFAP, A2B5, Sox2, and nestin, and differentiate into ScNs expressing neuronal markers TUJ1, NF, NeuroD, and NeuN. ScNs expressed glutamatergic marker VGLUT1, suggesting that ScNs are glutamatergic neurons. BDNF was capable of stimulating SGN-NSCs to differentiate into ScNs and promoting ScNs to elongate neurite outgrowths. Patch clamp recordings demonstrated that ScNs possessed NaV and HCN channel properties, which were reported in native SGNs. Moreover, we found a novel approach of using ACM to induce ScNs to express synaptic proteins, indicating the potential of synaptogenesis.

Previous in vitro studies have shown that sphere forming cells can be isolated from postnatal [18,19,21] and adult [29,30] murine spiral ganglion. These sphere-forming cells differentiated into cells expressing neuronal protein TUJ1 and glial marker GFAP [19,29,30]. Additionally, postnatal mouse utricle-derived cells showed neuronal-like features [20], including the expression of TUJ1 protein. Our data are consistent with previous studies, in which SGN-derived spheres expressed NSC proteins Sox2 and nestin, indicating that they possessed NSC features. The other property of NSC is proliferation, our EdU study suggested that ScN was able to incorporate EdU and proliferated in culture. In this study, majority of ScNs were bipolar neurons expressing VGLUT1, indicating ScNs are bipolar glutamatergic neurons, the correct neuron type for SGN replacement. To increase the generation of ScNs, neurotrophin BDNF was used in this study, as neurotrophins were reported to affect survival and neurogenesis of auditory neurons during development [31], and. We also explored whether BDNF was able to stimulate the generation of glutamatergic neurons, and we found that the percentage of VGLUT1-positive cells (VGLUT1/TUJ1) was not statistically different between the control and BDNF groups.

In the auditory system, the somata of SGNs locate in the modiolus of the inner ear with relatively long central processes (the cochlear nerve) connecting the cochlear nucleus in the brainstem [32]. Therefore, regeneration of neurite outgrowth is an important aspect in stem cell-based SGN replacement. However, this important question has not been explored previously. To address this issue, we characterized the number and length of neurite outgrowth of SGN-NSC-derived ScNs in this study. When BDNF was added to the ScN culture, statistical analysis showed no significant difference in the number of neurite outgrowths between the control and BDNF groups. However, when we measured the length of ScN neurite outgrowths, we found statistically significant longer neurite outgrowths extending from ScNs in cultures supplemented with BDNF, indicating that BDNF was able to stimulate the elongation of neurite outgrowths. Identification of methods to stimulate elongation of neurite outgrowth is critical for SGN replacement because it helps reconstructing the auditory pathway from the peripheral inner ear to the central cochlear nucleus.

Previous studies have characterized the morphological and protein expression of rodent inner ear tissue-derived neuron-like cells [18–20,29]. One study reported the electrophysiology features of mouse utricle-derived neuronal-like cells [20]. However, the function of spiral ganglion NSC-derived neurons has not been fully characterized. To determine whether stem cell-derived neurons possess the capability to substitute SGN, it is fundamental to study whether newly generated neurons are excitable and demonstrate electrophysiology features similar to native SGNs. In this study, we found that SGN-NSC-derived ScNs exhibited action potentials that involved both TTX-sensitive and TTX-insensitive NaV channels. Additionally, ScNs expressed HCN channels that were capable of generating $I_h$ current, which could be reversibly blocked by administration of cesium and involved the kinetically slower HCN subunits. These NaV channels and HCN channels are also found in native SGNs as reported previously [23–27]. The electrophysiology data in this study suggested that (1) ScNs generated in our study are electrophysiologically functional neurons; and (2) ScNs are SGN-like neurons, as they express SGN-like ion channels. Therefore, we demonstrate that ScNs are excitable neurons that possess SGN-like electrophysiology characteristics including NaV channels and HCN channels.

In the mammalian auditory system, SGNs form synapses with sensory receptors (hair cells) and brainstem cochlear nucleus to conduct sound signals. Therefore, a successful stem cell-based SGN regeneration must include synapse formation assays. However, synaptic formation assay has been rarely reported in the inner ear NSC studies. In this study, we initiated the synaptogenesis study in stem cell-based SGN regeneration by investigating the expression of synaptic proteins in SGN-NSC-derived cells. We found neuron–neuron contacts between ScNs in adherent cultures. Neurotrophin including BDNF did not appear to be able to remarkably stimulate the expression of synaptic proteins in ScNs.

In the neural system, astrocytes act as neuronal neighbors and support neuron function [33]. ACM obtained from astrocyte culture contains various nutrients, growth factors, and cytokines. The concentration of BDNF in the ACM is $\sim$50 pg/mL [34], whereas 20 ng/mL of BDNF was used for neuronal induction in this study, which is 400-folds difference. Additionally, western blotting shows that BDNF protein expression is not detected in ACM. Previous study showed that both astrocytes and ACM were able to promote the expression of synaptic proteins in the rat retina ganglia (the central nervous system) [35]. However, whether ACM is able to stimulate stem cell-derived neurons to express synaptic proteins is still obscure. In this study, ACM was collected from mouse astrocyte cultures and added to ScN cultures. We found that ACM was able to stimulate the expression of synaptic proteins in ScNs. This study suggests that tissue specific NSC-derived neurons possess the capability to form synapses and that ACM is able to stimulate synaptogenesis in stem cell-derived neurons. The weakness of this study is that we did not study the effect of ACM on neuronal marker TUJ1 expression. The reason is that BDNF is not detected in ACM using western blotting, which does not warrant the neuronal differentiation study to compare with the BDNF (control) study. In the meanwhile, it is possible that ACM contains growth factors and/or cytokines that may promote or inhibit or does not have any effect on neuronal marker TUJ1 expression, which is beyond the scope of current study, and may deserve independent studies in the future.

In summary, we identified and induced tissue-specific SGN-NSCs to differentiate into ScNs that showed electrophysiology features similar to native neurons. We found that

BDNF was able to stimulate the elongation of neurite outgrowths from ScNs, which is important for regeneration of neural connections in the auditory system. Moreover, we investigated the synaptogenesis of stem cell-derived neurons and discovered that ACM is able to stimulate the expression of synaptic proteins. We have demonstrated that SGN-NSC-derived neurons are excitable in electrophysiology and possess the synapse formation ability, which is fundamental to a successful auditory neuron replacement. The results of this study provide insights into neuronal regeneration using stem cell-based approaches, which open avenues to develop novel stem cell-based approaches to replace damaged SGNs and other sensory neurons in the peripheral sensory systems.

## Acknowledgments

This study is supported by NIH grant R01DC013275 to ZH and MH43987 to RA. We thank Yiyun Jiang, Xin Deng, Zhenjie Liu, and Yaozhu Leng for valuable comments to the article. Antibodies are from The Developmental Studies Hybridoma Bank and NeuroMab.

## Author Disclosure Statement

No competing financial interests exist.

## References

1. Wu SH and D Oertel. (1987). Maturation of synapses and electrical properties of cells in the cochlear nuclei. Hear Res 30:99–110.
2. Hernandez-Zamora E and A Poblano. (2014). [The auditory pathway: levels of integration of information and principal neurotransmitters]. Gac Med Mex 150:450–460.
3. WHO. (2012). WHO global estimates on prevalence of hearing loss. Mortality and Burden of Diseases and Prevention of Blindness and Deafness. www.who.int/pbd/deafness/WHO_GE_HL.pdf
4. Shepherd RK, A Coco and SB Epp. (2008). Neurotrophins and electrical stimulation for protection and repair of spiral ganglion neurons following sensorineural hearing loss. Hear Res 242:100–109.
5. Kujawa SG and MC Liberman. (2009). Adding insult to injury: cochlear nerve degeneration after ''temporary'' noise-induced hearing loss. J Neurosci 29:14077–14085.
6. Hoeffding V and ML Feldman. (1988). Changes with age in the morphology of the cochlear nerve in rats: light microscopy. J Comp Neurol 276:537–546.
7. Vartiainen E, S Karjalainen and J Karja. (1985). Auditory disorders following head injury in children. Acta Otolaryngol 99:529–536.
8. Bixenstine PJ, MP Maniglia, A Vasanji, KN Alagramam and CA Megerian. (2008). Spiral ganglion degeneration patterns in endolymphatic hydrops. Laryngoscope 118:1217–1223.
9. Schachern PA, DA Shea, MM Paparella and TH Yoon. (1989). Otologic histopathology of Fabry's disease. Ann Otol Rhinol Laryngol 98:359–363.
10. Satya-Murti S, A Cacace and P Hanson. (1980). Auditory dysfunction in Friedreich ataxia: result of spiral ganglion degeneration. Neurology 30:1047–1053.
11. Hu Z and M Ulfendahl. (2006). Cell replacement therapy in the inner ear. Stem Cells Dev 15:449–459.
12. Hu Z, D Wei, CB Johansson, N Holmström, M Duan, J Frisén and M Ulfendahl. (2005). Survival and neural differentiation of adult neural stem cells transplanted into the mature inner ear. Exp Cell Res 302:40–47.
13. Reyes JH, KS O'Shea, NL Wys, JM Velkey, DM Prieskorn, K Wesolowski, JM Miller and RA Altschuler. (2008). Glutamatergic neuronal differentiation of mouse embryonic stem cells after transient expression of neurogenin 1 and treatment with BDNF and GDNF: in vitro and in vivo studies. J Neurosci 28:12622–12631.
14. Chen W, N Jongkamonwiwat, L Abbas, SJ Eshtan, SL Johnson, S Kuhn, M Milo, JK Thurlow, PW Andrews, et al. (2012). Restoration of auditory evoked responses by human ES-cell-derived otic progenitors. Nature 490:278–282.
15. Bas E, TR Van De Water, V Lumbreras, S Rajguru, G Goss, JM Hare and BJ Goldstein. (2014). Adult human nasal mesenchymal-like stem cells restore cochlear spiral ganglion neurons after experimental lesion. Stem Cells Dev 23:502–514.
16. Yuan Y, Y Wang and F Chi. (2014). Reinnervation of hair cells by neural stem cell-derived neurons. Chin Med J (Engl) 127:2972–2976.
17. Zhang L, H Jiang and Z Hu. (2011). Concentration-dependent effect of nerve growth factor on cell fate determination of neural progenitors. Stem Cells Dev 20: 1723–1731.
18. Diensthuber M, V Zecha, J Wagenblast, S Arnhold, AS Edge and T Stöver. (2014). Spiral ganglion stem cells can be propagated and differentiated into neurons and glia. Biores Open Access 3:88–97.
19. Oshima K, DT Teo, P Senn, V Starlinger and S Heller. (2007). LIF promotes neurogenesis and maintains neural precursors in cell populations derived from spiral ganglion stem cells. BMC Dev Biol 7:112.
20. Martinez-Monedero R, E Yi, K Oshima, E Glowatzki and AS Edge. (2008). Differentiation of inner ear stem cells to functional sensory neurons. Dev Neurobiol 68:669–684.
21. Oshima K, P Senn and S Heller. (2009). Isolation of sphere-forming stem cells from the mouse inner ear. Methods Mol Biol 493:141–162.
22. Villalobos C, RC Foehring, JC Lee and R Andrade. (2011). Essential role for phosphatidylinositol 4,5-bisphosphate in the expression, regulation, and gating of the slow after-hyperpolarization current in the cerebral cortex. J Neurosci 31:18303–18312.
23. Szabo ZS, CS Harasztosi, I Sziklai, G Szucs and Z Rusznak. (2002). Ionic currents determining the membrane characteristics of type I spiral ganglion neurons of the guinea pig. Eur J Neurosci 16:1887–1895.
24. Mo ZL and RL Davis. (1997). Endogenous firing patterns of murine spiral ganglion neurons. J Neurophysiol 77: 1294–1305.
25. Bakondi G, A Por, I Kovacs, G Szucs and Z Rusznak. (2009). Hyperpolarization-activated, cyclic nucleotide-gated, cation non-selective channel subunit expression pattern of guinea-pig spiral ganglion cells. Neuroscience 158:1469–1477.
26. Chen C. (1997). Hyperpolarization-activated current (Ih) in primary auditory neurons. Hear Res 110:179–190.
27. Biel M, C Wahl-Schott, S Michalakis and X Zong. (2009). Hyperpolarization-activated cation channels: from genes to function. Physiol Rev 89:847–885.
28. Iwabuchi S, Y Kakazu, JY Koh, KM Goodman and NC Harata. (2014). Examination of synaptic vesicle recycling using FM dyes during evoked, spontaneous, and miniature synaptic activities. J Vis Exp 85:e50557–e50557.

29. Rask-Andersen H, M Bostrom, B Gerdin, A Kinnefors, G Nyberg, T Engstrand, JM Miller and D Lindholm. (2005). Regeneration of human auditory nerve. In vitro/in video demonstration of neural progenitor cells in adult human and guinea pig spiral ganglion. Hear Res 203:180–191.
30. Oshima K, CM Grimm, CE Corrales, P Senn, R Martinez Monedero, GS Geleoc, A Edge, JR Holt and S Heller. (2007). Differential distribution of stem cells in the auditory and vestibular organs of the inner ear. J Assoc Res Otolaryngol 8:18–31.
31. Leake PA, O Stakhovskaya, A Hetherington, SJ Rebscher and B Bonham. (2013). Effects of brain-derived neurotrophic factor (BDNF) and electrical stimulation on survival and function of cochlear spiral ganglion neurons in deafened, developing cats. J Assoc Res Otolaryngol 14: 187–211.
32. Hu Z. (2013). Formation of the peripheral-central transitional zone in the postnatal mouse cochlear nerve. Otolaryngol Head Neck Surg 149:296–300.
33. Haydon PG. (2001). GLIA: listening and talking to the synapse. Nat Rev Neurosci 2:185–193.
34. Yang Q, B Feng, K Zhang, Y Guo, S Liu, Y Wu, X Li and M Zhao. (2012). Excessive astrocyte-derived neurotrophin-3 contributes to the abnormal neuronal dendritic development in a mouse model of fragile X syndrome. PLoS Genet 8:e1003172.
35. Christopherson KS, EM Ullian, CC Stokes, CE Mullowney, JW Hell, A Agah, J Lawler, DF Mosher, P Bornstein and BA Barres. (2005). Thrombospondins are astrocyte-secreted proteins that promote CNS synaptogenesis. Cell 120:421–433.

Address correspondence to:
*Dr. Zhengqing Hu*
*Department of Otolaryngology-HNS*
*Wayne State University School of Medicine*
*550 East Canfield Street, 258 Lande*
*Detroit, MI 48201*

*E-mail:* zh@med.wayne.edu

Received for publication November 3, 2015
Accepted after revision March 24, 2016
Prepublished on Liebert Instant Online March 28, 2016